Available online at www.sciencedirect.com
SCIENCE DIRECT®
Chemical Physics Letters 387 (2004) 209–215
CHEMICAL PHYSICS LETTERS
www.elsevier.com/locate/cplett

Enzyme functionality and solvation of Subtilisin *Carlsberg*: from hours to femtoseconds

J.K. Amisha Kamal, Tianbing Xia, Samir Kumar Pal, Liang Zhao, Ahmed H. Zewail *

Laboratory for Molecular Sciences, Arthur Amos Noyes Laboratory of Chemical Physics, California Institute of Technology, Pasadena, CA 91125, USA

Received 12 January 2004
Published online: 6 March 2004

Abstract

We report studies of the enzymatic activity of Subtilisin *Carlsberg* (SC) in different solvents and pH's using two substrates. From the Michaelis–Menten mechanism, we found the specificity constant (k_{cat}/K_M) of enzymatic activity to be retarded when organic solvents, such as acetonitrile or dioxane, are added to the aqueous medium or when the pH is lowered. In order to address the role of solvation, we also studied the femtosecond dynamics of the enzyme and the solubility of substrates and products. We elucidate the nature of the free energy surface from the knowledge of the free energy change (K_M), catalytic turn over (k_{cat}), solvation, and effect of pH on the enzymatic activity.

1. Introduction

The application of organic solvents in enzymatically catalyzed reactions has gained increasing importance [1–3]. It has been shown that catalytic activity decreases in the presence of an organic solvent [4]. Adding small quantities of water, thus ensuring the existence of a partial hydration layer around the enzyme molecule, accelerates the catalytic rate, yet much below to that in pure aqueous medium [5]. A low enzymatic activity can be a result of various factors: (i) diffusional and accessibility limitations, (ii) structural changes and conformational flexibility, (iii) change in the mechanistic pathway and pK_a of the active site residue(s) and (iv) altered energetics of reactants, transition states and products [4]. Most of the water miscible organic solvents act as denaturants (e.g. dimethyl sulfoxide, dimethyl formamide, etc.). They unfold the enzyme and retard the activity. Water miscible organic solvents that have less denaturing effect (e.g. acetonitrile, dioxane, etc.) also reduce the enzymatic activity significantly, the mechanism of which has been the focus of numerous publications in the recent past [4–6]. It has been suggested that these organic solvents primarily interact with the enzyme-bound water layer rather than the enzyme itself [5].

In the present study, we measured the activity of the enzyme, Subtilisin *Carlsberg* (SC) using two substrates, Ala-Ala-Phe-7-amido-4-methyl coumarin (AAF-AMC) and succinyl-Ala-Ala-Pro-Phe-*p*-nitroanilide (Suc-AAPF-*p*NA) in different binary aqueous-organic solvents and at different pH's. SC is a serine protease whose physiological role is to hydrolyze proteins. Fig. 1 shows the schematic structures of SC and the substrates used. The active site residues (Ser221, His64, Asp32), otherwise called *catalytic triad*, are indicated. Using the single tryptophan (Trp113) at the surface of the protein (Fig. 1) as a probe, we measured femtosecond and picosecond solvation dynamics in the same aqueous-organic solvent mixtures and in the buffer at pH = 4.5; measurements of solvation dynamics of the enzyme SC in aqueous buffer at pH = 7.0 have been reported previously from this lab [7]. Solubility of substrates and products was carried out to probe the solvent effect on their ground state free energy.

* Corresponding author. Fax: +1-626-792-8456.
E-mail address: zewail@caltech.edu (A.H. Zewail).

0009-2614/$ - see front matter © 2004 Elsevier B.V. All rights reserved.
doi:10.1016/j.cplett.2004.02.011

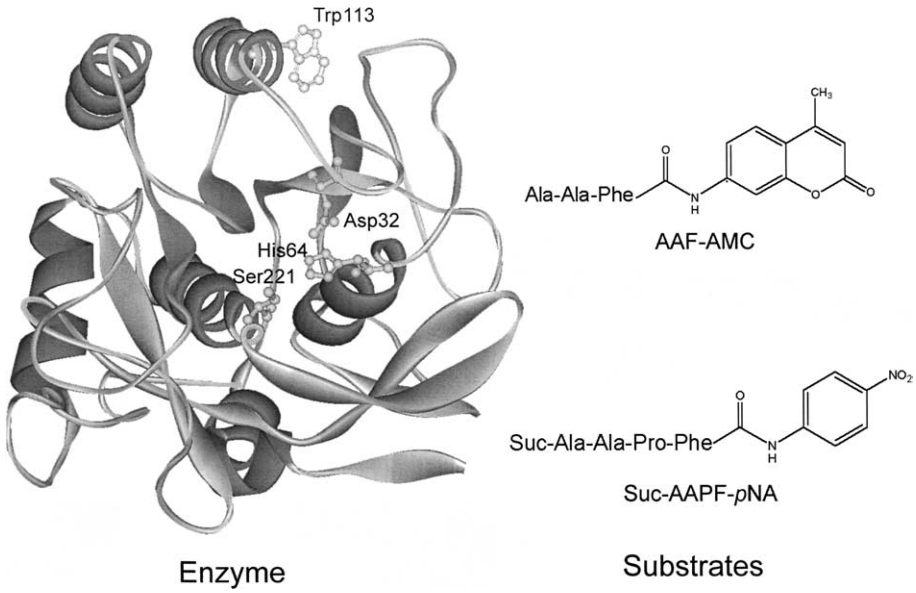

Fig. 1. Schematic structures of the enzyme, Subtilisin *Carlsberg* (SC) and the substrates, Ala-Ala-Phe-7-amido-4-methyl coumarin (AAF-AMC) and succinyl-Ala-Ala-Pro-Phe-*p*-nitroanilide (Suc-AAPF-*p*NA). The positions of the single tryptophan residue (Trp113) and the catalytic triad in the active site (Ser221, His64, and Asp32) are indicated.

2. Experimental

Subtilisin *Carlsberg* (SC), acetonitrile (ACN), Ala-Ala-Phe-7-amido-4-methyl coumarin (AAF-AMC), succinyl-Ala-Ala-Pro-Phe-*p*-nitroanilide (Suc-AAPF-*p*NA), and N-Acetyl-L-tryptophanamide (NATA) were purchased from Sigma. Dioxane (DX) was from EM Science. 7-amino-4-methyl coumarin (AMC) and *p*-nitroaniline (*p*NA) were purchased from Molecular Probes and Alfa Aesar, respectively. Aqueous-organic solutions (40% ACN, 50% DX, v/v) were prepared in a phosphate buffer (final concentration is 50 mM) at pH = 7.0. For the activity experiments with Suc-AAPF-*p*NA, the buffer used to prepare aqueous-organic solvent mixtures was 20 mM Tris–HCl and the pH was adjusted to 7.8, since phosphate buffer at pH = 7.0 caused detectable spontaneous hydrolysis of the substrate. Acetate buffer (50 mM) was used for protein solutions at pH = 4.5. Concentrations of the enzyme samples in aqueous solution were determined using the reported extinction coefficient value at 280 nm, $\varepsilon_{280} = 23.46\ \text{mM}^{-1}\ \text{cm}^{-1}$ [8]. Solubility measurements of the substrates and products were carried out at room temperature (23 °C).

Circular dichroism (CD) data were recorded on an AVIV 62A-DS spectropolarimeter equipped with a thermo-electric setup using a rectangular cell of 1 mm path length. Percentage of helical content was computed using the reported computer program [9]. Thermal unfolding of SC was monitored by recording CD at 222 nm as a function of temperature. The temperature was raised from 1 to 99 °C in 1 °C step with 1 or 2 min equilibration time at each temperature. The unfolding curves were constructed after converting the CD values to fraction unfolded [10].

Catalytic activity measurements of SC were made using the chromogenic synthetic substrates AAF-AMC and Suc-AAPF-*p*NA as per the conventional procedure [11,12]. Concentrations of the substrates were determined using $\varepsilon_{325} = 16\ \text{mM}^{-1}\ \text{cm}^{-1}$ for AAF-AMC in buffer pH = 7.0, and $\varepsilon_{315} = 14\ \text{mM}^{-1}\ \text{cm}^{-1}$ for Suc-AAPF-*p*NA in water. Increase in the absorption at 370 nm for the release of AMC and that at 410 nm for the release of *p*NA were monitored as a function of time (in 1 cm cell) using a Varian Cary 500 spectrophotometer. The enzyme concentration was held constant, in the range 10–40 μM and 0.005–1 μM for reaction with AAF-AMC and Suc-AAPF-*p*NA, respectively, for each kinetic measurement. Initial rates were calculated from the slope of the linear region of the absorbance change with time (1–10 min) and using the extinction coefficient values of the products. For AMC, $\varepsilon_{370} = 7.6\ \text{mM}^{-1}\ \text{cm}^{-1}$ (aqueous buffer), $8.9\ \text{mM}^{-1}\ \text{cm}^{-1}$ (40% ACN) and $10.2\ \text{mM}^{-1}\ \text{cm}^{-1}$ (50% DX); for *p*NA, $\varepsilon_{410} = 8.8\ \text{mM}^{-1}\ \text{cm}^{-1}$ (aqueous buffer and 50% DX) and $8.2\ \text{mM}^{-1}\ \text{cm}^{-1}$ (40% ACN); all obtained from the absorption of the pure compounds. The values of the apparent enzyme–substrate dissociation constant (K_M) and *catalytic turnover number* (k_{cat}) were derived by least squares fitting of the double reciprocal Lineweaver–Burk plot [12] assuming the enzyme to be 100% functional (no side channels).

For the femtosecond dynamics measurements, the experimental setup is as described elsewhere [13]. Briefly, a femtosecond (fs) pulse (~200 nJ) was used to excite the

tryptophan at 297 nm. Fluorescence was detected using the up-conversion method. Data analysis follows that reported in [13], and references therein. The reported correlation function, $C(t)$, provides the temporal evolution of solvation, basically describing the rotational and translational motions of the solvent around the solute.

3. Results and discussion

3.1. Enzyme kinetics

In Fig. 2a, we show the spectral characteristics of the substrate, AAF-AMC (S), and the product, AMC (P). The time courses of increase in the absorbance at 370 nm (up to 80 min) for hydrolysis of AAF-AMC are given in Fig. 2b. The behavior shown elucidates the general effect of solvation and pH. In Fig. 3, we present the Lineweaver–Burk plots ($[E]_0/v$ versus $1/[S]_0$, where $[E]_0$ is the initial enzyme concentration, v is the initial reaction rate, and $[S]_0$ is the initial substrate concentration) for the activity of the enzyme SC with the substrates AAF-AMC and Suc-AAPF-*p*NA under different reaction conditions. The activity parameters obtained in aqueous medium for these substrates at near neutral pH (Table 1) broadly agrees with those reported for subtilisin from *amyloliquefaciens* and α-chymotrypsin [14,15].

Table 1 shows that the 'apparent bimolecular rate constant' (k_{cat}/K_M) decreased by 2–3 orders of magnitude in 40% ACN or 50% DX and when pH is lowered to 4.5. Clearly, the effect of adding organic solvent and lowering the pH is the retardation of the catalytic efficiency of SC. For the case of organic co-solvent, an increase in the K_M value of 2 orders of magnitude was largely responsible for the decreased efficiency (Table 1). The k_{cat} for AAF-AMC appeared largely unaffected (or slightly increased). A similar trend of increasing K_M (18 ± 3 to 170 ± 110 mM) and nearly unaffected k_{cat} ($V_{max} = 0.88 \pm 0.06$ and 1.2 ± 0.6 μM s^{-1} for a constant E_0) was observed for enzymatic activity of SC with phenyl acetate when the medium was changed from buffer pH = 7.8 to glycerol containing 1% (v/v) water

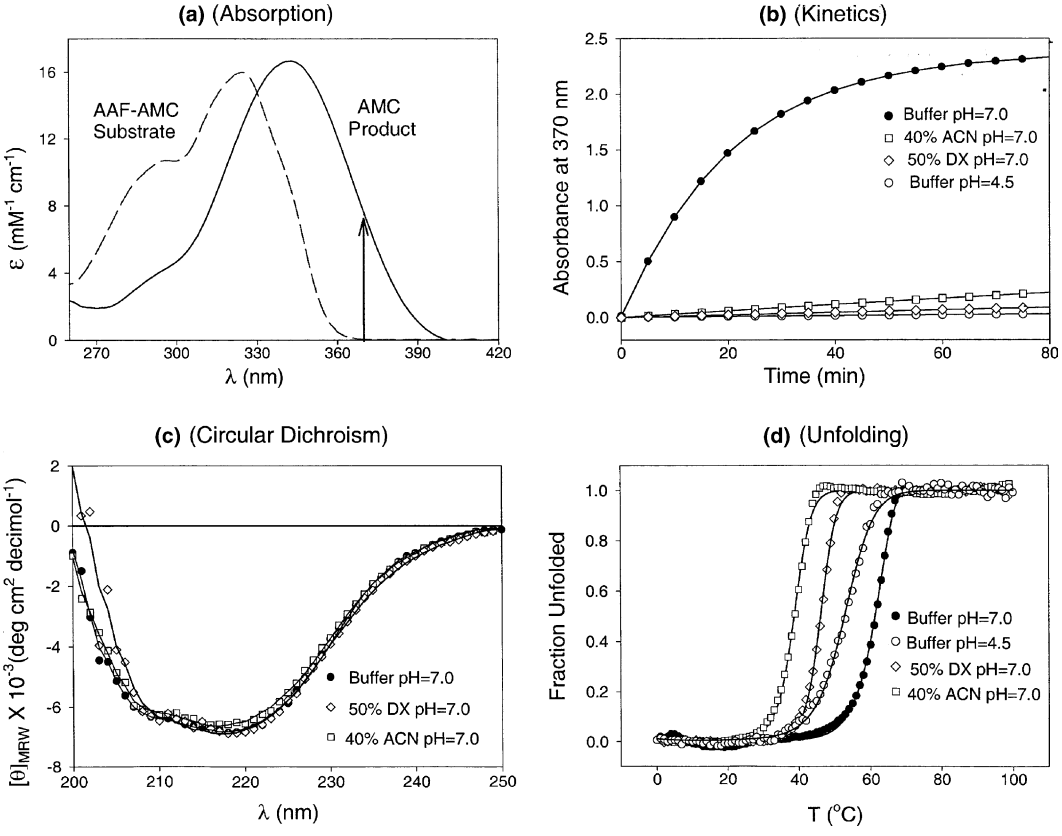

Fig. 2. (a) Spectral characteristics of substrate (S), AAF-AMC and the product (P), AMC. Arrow indicates the wavelength (370 nm) used for monitoring the enzyme kinetics with substrate AAF-AMC. (b) The absorbance at 370 nm as a function of time. Concentrations of SC and AAF-AMC were 40 and 500 μM, respectively. (c) Far UV-CD spectra of SC. Mean residue ellipticity ($[\theta]_{MRW}$) was calculated from $CD/(10 \times C \times l \times N)$ where *CD* is the observed CD in milli-degrees, *C* is the molar concentration, *l* is the path length in centimetres and *N* is the number of amino acid residues (274 for SC). The fits to the data points are the computed spectra according to [9] for estimation of helical content. (d) Thermal unfolding curves of SC in different solvent conditions. Transition temperatures (T_m, the midpoint of unfolding transition) are 62, 53, 46, 39 °C for SC in buffer pH = 7.0, in buffer pH = 4.5, in 50% DX, and in 40% ACN, respectively.

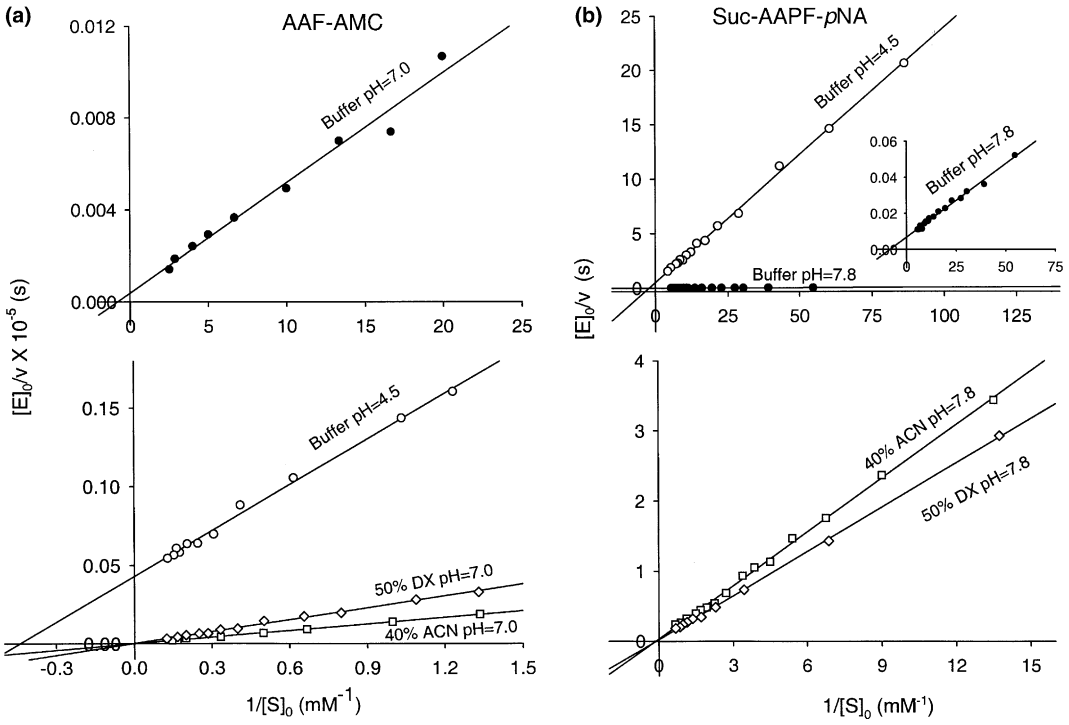

Fig. 3. (a) Lineweaver–Burk plots of SC showing its catalytic activity with AAF-AMC in (●) 50 mM phosphate buffer pH = 7.0, (□) 40% ACN pH = 7.0, (△) 50% DX pH = 7.0, and (○) 50 mM acetate buffer pH = 4.5. (b) Similar plots for Suc-AAPF-*p*NA in (●) 20 mM Tris–HCl buffer pH = 7.8, (□) 40% ACN pH = 7.8, (△) 50% DX pH = 7.8, and (○) 50 mM acetate buffer pH = 4.5. The plot for buffer pH = 7.8 is redrawn as inset figure, for clarity.

Table 1
Kinetic parameters for the activity of the enzyme Subtilisin *Carlsberg* with two substrates, AAF-AMC and Suc-AAPF-*p*NA at 23 °C

Solvent[a]	Enzymatic hydrolysis of AAF-AMC			Solubility (mM)[b]	
	K_M (mM)	k_{cat} (s^{-1})	k_{cat}/K_M ($M^{-1}\,s^{-1}$)	AAF-AMC	AMC
Buffer pH = 7.0	0.9 ± 0.1	0.019 ± 0.002	21.1 ± 3.2	2	0.25
40% Acetonitrile pH = 7.0	113 ± 23	0.066 ± 0.03	0.58 ± 0.29	80	10
50% Dioxane pH = 7.0	181 ± 10	0.048 ± 0.02	0.27 ± 0.11	94	26
Buffer pH = 4.5	2.1 ± 0.2	0.0002 ± 0.00002	0.10 ± 0.01	37	0.34
	Enzymatic hydrolysis of Suc-AAPF-*p*NA			Suc-AAPF-*p*NA	*p*NA
Buffer pH = 7.8	0.12	144	1.2×10^6	5.0	3.3
40% Acetonitrile pH = 7.8	11.3	44	3.9×10^3	34	104
50% Dioxane pH = 7.8	12.0	57	4.8×10^3	64	175
Buffer pH = 4.5	0.45	2	4.2×10^3	0.4	3.3

Also given are the solubility of substrates and products at 23 °C. For AAF-AMC, the K_M and k_{cat} values are average of duplicate measurements with different enzyme concentrations.

[a] Polarity decreases in the order, water > acetonitrile > dioxane.

[b] Solubility is determined from the absorption of the supernatant of the saturated solution.

[16]. For the second substrate, Suc-AAPF-*p*NA, a decrease in k_{cat} (3-fold) accompanied the large increase in the K_M.

The situation is somewhat different for the behavior at two different pH's. The predominant effect of lowering pH was the reduction of k_{cat} value by the same order of magnitude as that of k_{cat}/K_M. Clearly, the retarded efficiency at low pH is largely due to retarded *catalytic turn over*. It is reported that, at lower pH, protonation of histidine of the *catalytic triad* (His64, $pK_a = 7.0$) occurs, which reduces the k_{cat} value [13,17–19]. The variation of K_M was reported to be pH independent over the range of pH 6.0–9.0 [17,18]. When pH is lowered from 7.0 to 4.5, we observed a reproducible 2-fold increase in the K_M for AAF-AMC. The increase in K_M for Suc-AAPF-*p*NA was 4-fold for a pH change from 7.8 to 4.5. This indicates a pH dependent K_M below the value of pH = 6.0. To confirm our results, we measured the hydrolysis of

AAF-AMC at two other pH's, above and below pH = 6.0: at pH = 6.3, $K_M = 0.89$ mM and $k_{cat} = 0.004$ s^{-1}; at pH = 5.5, $K_M = 2.0$ mM and $k_{cat} = 0.002$ s^{-1}. The K_M at pH 6.3 is similar to that at pH 7.0, but that at pH 5.5 is 2-fold lower, thus corroborating our findings. This abrupt increase in K_M between pH = 6.0 and 5.5 after which the increase is constant up to pH 4.5 is less likely due to protonation in the substrate (based on the expected pK_a of substrate, Fig. 1).

3.2. Solvation dynamics

Before proceeding to obtain solvation dynamics of Trp in the enzyme, we first studied a mimic (NATA) of the substrate (peptide) using Trp as a probe. The behavior of solvent correlation functions are given in Fig. 4a, together with that of free Trp in bulk water [7]. In general, for all the solvent conditions τ_1 was in the range of 0.1–0.3 ps and τ_2 was in the range of 1.0–1.6 ps. For 50% DX, a third longer component $\tau_3 = 26$ ps was observed. This value is similar to that reported previously for another probe (coumarin 153) in pure DX (18.3 ps) [20]. All these features are typical of probe

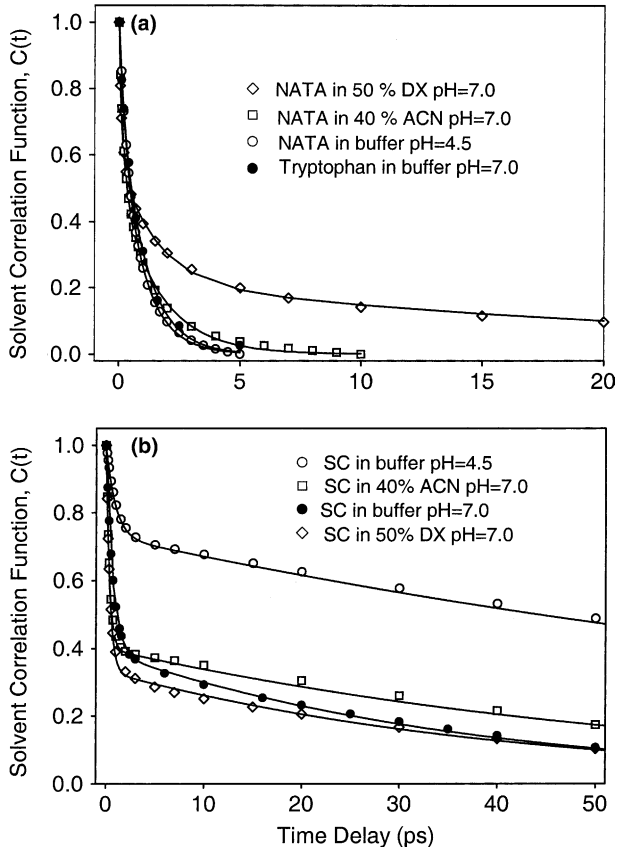

Fig. 4. (a) Comparison of the decays of solvent correlation functions of NATA under various solvent conditions. (b) Comparison of the decays of solvent correlation functions of SC. The result for buffer pH = 7.0 [7] is shown in both figures for comparison with the physiological condition.

experiencing a bulk solvation, as it has been discussed earlier [7,21], and provide time scales of substrate solvation.

For tryptophan in the enzyme SC, the fittings of $C(t)$ shown in Fig. 4b gave two time constants. These fast and slow components describe the corresponding dynamics of 'bulk type' and 'bound type' solvent molecules [7]. The long time constant in 40% ACN is $\tau_2 = 50$ ps (45%) and in 50% DX is $\tau_2 = 42$ ps (45%). These are similar to the values (38 ps, 39%) at pH = 7.0 [7], but different from that of tryptophan or NATA, as discussed above. However, when the enzyme is at pH = 4.5, the results show a significantly longer $\tau_2 = 110$ ps (68%).

3.3. Dynamics, function and the energy landscape

From structural point of view, the far UV-CD (200–250 nm) spectra for SC in buffer (pH = 7.0), 40% ACN and 50% DX (Fig. 2c) provide the helical content which remains at 34% (±1) and agrees with the X-ray structural data (33%) [22]. This confirms the intactness of the protein secondary structure. Active site titration experiments of SC indicated a nearly intact *catalytic triad* in aqueous and organic solvents [23]. Further, we observed single-step equilibrium thermal unfolding curves for SC with distinct native baselines up to 30 °C (Fig. 2d). Taken together, these results suggest that the structure of SC remains in the native form in the solvents studied at room temperature. It is reported that the diffusion and accessibility, catalytic mechanism, the pH profile, and the transition state structure of SC are not significantly affected by the presence of organic co-solvent [4,6]. In this light of understanding, altered enzymatic activity offers a unique opportunity for correlating the function with the dynamics.

The trends reported here for the effect of solvation and pH can be understood by relating the function of the enzyme to changes on the free energy profile, as depicted in Fig. 5. The altered energetics of the enzyme–substrate complexation and that of the *catalytic turn over* are the keys to determine changes in the free energy. From the scheme in Fig. 5 and the results in Fig. 3, it can be shown that the observed enzyme kinetics follows Michaelis–Menten mechanism. The measured k_{cat} divided by k_1 (diffusion controlled, 10^7–10^9 $M^{-1}\,s^{-1}$) is nearly zero, indicating that K_M is the dissociation equilibrium constant. For the substrate–enzyme entrance channel, the free energy is $\Delta G_S = -RT \ln(1/K_M)$, while in the exit channel, it is given by $\Delta G^{\ddagger} = -RT \ln(k_{cat} \times h/kT)$; the overall activation is given by $\Delta G_T^{\ddagger} = -RT \ln(k_{cat}/K_M \times h/kT)$ [12].

When the reaction medium for the hydrolysis of Suc-AAPF-*p*NA, is changed from water to 40% ACN or 50% DX, the overall activation energy barrier is increased by 3.2–3.4 kcal mol^{-1} (from the data in Table 1). The binding free energy (ΔG_S) decreases by 2.7

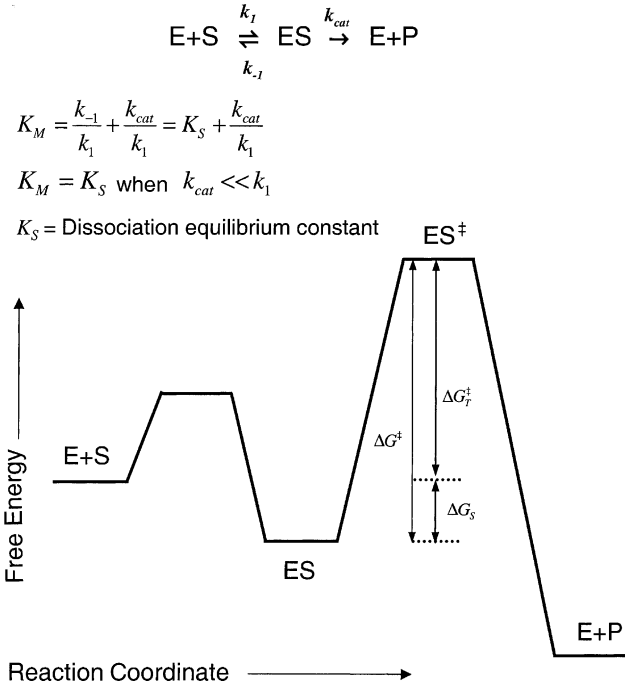

Fig. 5. Free energy profile for the enzymatic activity. E, S, P, ES and ES‡ denote the enzyme, substrate, product, enzyme–substrate complex, and transition state respectively.

kcal mol^{-1}. In other words, the reduced enzyme–substrate complexation accounts for ~80% of the retarded catalytic efficiency. The complexation is reduced when there are (i) solvation (ground state stabilization) of the substrate and the enzyme, and (ii) desolvation (ground state destabilization) of the ES [3]. The solvation of substrate Suc-AAPF-*p*NA ($-RT\Delta \ln S$, where S is the solubility [24]) amounts to 1.1–1.5 kcal mol^{-1} as calculated from its solubility's (from Table 1), which accounts for ~50% of the reduced complexation. It is reported that enzymes are usually desolvated in organic co-solvent [25]. This leads to desolvation of ES, which also contributes to the reduced complexation.

The 3-fold decrease in k_{cat}, in 40% ACN or 50% DX, for the hydrolysis of Suc-AAPF-*p*NA represents the interplay of desolvation of the ES species and that of the transition state, and the possible restriction on conformational flexibility. The transition state (ES‡) is polar [12,24] and the presence of ACN or DX in the active site [26] could desolvate the ES‡. As for the flexibility, reported time resolved fluorescence anisotropy studies of SC has indicated that the enzyme flexibility (nanosecond segmental mobility) decreases in the presence of organic co-solvent [27]. On the timescale of our observed solvation, major conformational changes are not expected. In the case of substrate AAF-AMC, the k_{cat} was found to be very small and the trend with solvation must take into account the errors listed in Table 1.

For the pH change from 7.0 or 7.8 to 4.5, K_M increases by 2–4 fold and k_{cat} decreases by two orders of magnitude for both substrates (Table 1). Protonation of His64 [17–19] is an important factor in the decrease of k_{cat}. The solvation dynamics of the protein are relevant to the recognition process (entrance channel) and to the chemistry at the active site. For SC in binary aqueous-organic solvents, the timescale of solvation obtained is ~50 ps and, as mentioned above, the solvent layer around SC is relatively robust in the mixed solvents. For the pH change from 7.0 to 4.5, the hydration time constant changes from 38 ps to 110 ps. This increased rigidity of solvation has two major influences: the change in the effective barrier for *recognition* (E···S) and the restriction of the possible conformations of the ES complexes for *reactivity* (Fig. 5), both are significantly driven by the entropic changes. The effect on the energetics is also possible – the more ordered the water, the less stable (entropically) the E+S and the ES species. This entropic change would be manifested in the unfolding behavior (see Fig. 2d). The studies reported here should be extended to other enzymes.

Acknowledgements

This work is supported by National Science Foundation (NSF).

References

[1] F. Bordusa, Chem. Rev. 102 (2002) 4817.
[2] P.J. Halling, Enzyme Mcrob. Technol. 16 (1994) 178.
[3] J.S. Dordick, Biotechnol. Prog. 8 (1992) 259.
[4] A.M. Klibanov, Trends Biotechnol. 15 (1997) 97.
[5] A. Zaks, A.M. Klibanov, J. Biol. Chem. 263 (1988) 8017.
[6] C.R. Wescott, A.M. Klibanov, Biochim. Biophys. Acta 1206 (1994) 1, and references therein.
[7] S.K. Pal, J. Peon, A.H. Zewail, Proc. Natl. Acad. Sci. USA 99 (2002) 1763.
[8] F.S. Markland, E.L. Smith, in: P.D. Boyer (Ed.), The Enzymes, Academic Press, New York, 1971, p. 561.
[9] W.C. Johnson, Proteins Struct. Funct. Genet. 35 (1999) 307.
[10] J.K.A. Kamal, D.V. Behere, J. Biol. Chem. 277 (2002) 40717.
[11] G. Sarath, M.G. Zeece, A.R. Penheiter, in: R. Beynon, J.S. Bond (Eds.), Proteolytic Enzymes: Practical Approach, Oxford University Press, New York, 2001, p. 45.
[12] A. Fersht, Enzyme Structure and Mechanism, W.H. Freeman and Company, New York, 1999.
[13] S.K. Pal, J. Peon, A.H. Zewail, Proc. Natl. Acad. Sci. USA 99 (2002) 15297.
[14] A.J. Russell, A.R. Fersht, Nature 328 (1987) 496.
[15] E.G. Delmar, C. Largman, J.W. Brodrick, M.C. Geokas, Anal. Biochem. 99 (1979) 316.
[16] K. Xu, K. Griebenow, A.M. Klibanov, Biotechnol. Bioeng. 56 (1997) 485.
[17] A.N. Glazer, J. Biol. Chem. 242 (1967) 433.
[18] L. Polgar, M.L. Bender, Biochemistry 6 (1967) 610.
[19] J. Kraut, in: P.D. Boyer (Ed.), The Enzymes, Academic Press, New York, 1971, p. 547.
[20] M.L. Horng, J.A. Gardecki, A. Papazyan, M. Maroncelli, J. Phys. Chem. 99 (1995) 17311.

[21] D. Zhong, S.K. Pal, D. Zhang, S.I. Chan, A.H. Zewail, Proc. Natl. Acad. Sci. USA 99 (2002) 13.
[22] J.L. Schmitke, L.J. Stern, A.M. Klibanov, Proc. Natl. Acad. Sci. USA 94 (1997) 4250.
[23] A. Zaks, A.M. Klibanov, J. Biol. Chem. 263 (1988) 3194.
[24] J. Kim, D.S. Clark, J.S. Dordick, Biotechnol. Bioeng. 67 (2000) 112.
[25] J.T. Chin, S.L. Wheeler, A.M. Klibanov, Biotechnol. Bioeng. 44 (1994) 140.
[26] J.L. Schmitke, L.J. Stern, A.M. Klibanov, Biochem. Biophys. Res. Commun. 248 (1998) 273.
[27] J. Broos, A.J.W.G. Visser, J.F.J. Engbersen, W. Verboom, A. Van Hoek, D.N. Reinhoudt, J. Am. Chem. Soc. 117 (1995) 12654.